1996ApJ...456..902R

THE ASTROPHYSICAL JOURNAL, 456:902–908, 1996 January 10
No copyright claimed for this article. Printed in U.S.A.

OPAL EQUATION-OF-STATE TABLES FOR ASTROPHYSICAL APPLICATIONS

FORREST J. ROGERS
Lawrence Livermore National Laboratory, P.O. Box 808, Livermore, CA 94550
FRITZ J. SWENSON
Los Alamos Astrophysics, Los Alamos National Laboratory, X-2 MS B220, Los Alamos, NM 87545
AND
CARLOS A. IGLESIAS
Lawrence Livermore National Laboratory, P.O. Box 808, Livermore, CA 94550
Received 1995 May 15; accepted 1995 July 18

ABSTRACT

OPAL opacities have recently helped to resolve a number of long-standing discrepancies between theory and observation. This success has made it important to provide the associated equation-of-state (EOS) data. The OPAL EOS is based on an activity expansion of the grand canonical partition function of the plasma in terms of its fundamental constituents (electrons and nuclei). The formation of composite particles and many-body effects on the internal bound states occur naturally in this approach. Hence, pressure ionization is a consequence of the theory. In contrast, commonly used approaches, all of which are based on minimization of free energy, are forced to assert the effect of the plasma on composite particles and must rely on an ad hoc treatment of pressure ionization. Another advantage of the OPAL approach is that it provides a systematic expansion in the Coulomb coupling parameter that includes subtle quantum effects generally not considered in other EOS calculations.

Tables have been generated that provide pressure, internal energy, entropy, and a variety of derivative quantities. These tables cover a fairly broad range of conditions and compositions applicable to general stellar-evolution calculations for stars more massive than $\sim 0.8\ M_{\odot}$. An interpolation code is provided along with the tables to facilitate their use.

Subject headings: atomic data — atomic processes — equation of state

1. INTRODUCTION

The inability to resolve a number of long-standing discrepancies between theory and stellar observations led to the speculation that the widely used Los Alamos opacities were missing important sources of opacity (Simon 1982; Christensen-Dalsgaard et al. 1985). Because of this speculation and the need for the opacity of low-Z materials to model laser-produced plasmas, the OPAL opacity effort was undertaken (Iglesias, Rogers, & Wilson 1987, 1992; Iglesias & Rogers 1991a, b; Rogers & Iglesias 1992). While the development of a detailed equation of state (EOS) was necessary to calculate the occupation numbers needed for opacity calculations, the publication of EOS tables for astrophysical use was deferred because of the relatively large size of the tables required to calculate accurate derivatives of EOS quantities. Historically, stellar models have been computed inconsistently, since the EOS used to compute the opacities has had little if anything to do with that used throughout the rest of the model. The success of the OPAL opacities in helping to improve theoretical models (e.g., Moskalik, Buchler, & Marom 1992; Guenther et al. 1992; Swenson et al. 1994a, b) has made it essential to provide EOS data that is consistent with the already available opacity tables.

The simple ionization equilibrium model introduced by Saha (1920) led to a revolution in stellar modeling and is adequate for many purposes. However, the modeling of high-quality observational data requires much greater accuracy in the EOS. For example, to model helioseismic data, derivatives of the EOS must be accurate to better than 1% (Christensen-Dalsgaard & Däppen 1992), a level of precision that can only be expected from fundamental procedures. Saha's model assumes ideal-gas conditions and uses only the ground-state configuration in the ionization-balance equations. A complete model needs to treat all excited states, including many-body effects as well as nonideal corrections due to Coulomb interactions. These effects are interrelated, and as a result, ad hoc approaches are prone to count the same term twice (see § 3). Consequently, corrections to the Saha equation obtained by ad hoc approaches can vary by substantial amounts (gauged by stellar-modeling sensitivity).

Considerable effort has been devoted to the fundamental treatment of hydrogen plasmas. An in-depth description of much of this work can be found in the books by Kraeft et al. (1986) and Ebeling, Kraeft, & Kremp (1977; see also DeWitt 1966; Krasnikov 1977). The more general problem of multicomponent plasmas has received much less attention (Rogers 1994, 1986, 1981; Krasnikov & Kucherenko 1978; Ebeling 1974), although a new approach for treating multicomponent plasmas based on the Feynman-Kac path-integral representation has recently been developed (Alastuey & Perez 1992; Alastuey 1994).

Typical stellar-model calculations require the EOS for a large, variable set of temperature-density points and for variable composition. It is thus very desirable to have available an efficient model that allows on-line computation or, failing that, a model that can be used to produce tables. All such models in current use, including the Saha equation, are based on free-energy minimization methods. These approaches work in the *chemical picture* and deal explicitly with ions and atoms, i.e., assert the effect of the plasma on their internal structure. On

© American Astronomical Society • Provided by the NASA Astrophysics Data System

1996ApJ...456..902R

the other hand, ab initio treatments of the EOS of partially ionized plasmas consider explicitly the fundamental particles. These approaches are developed in the grand canonical ensemble and are known as *physical-picture* methods. The present work uses the activity-expansion method of Rogers (1994), used earlier to compute the OPAL opacity tables, to tabulate the stellar EOS. The various physical processes included in the OPAL EOS are detailed in § 3.

Tables have been constructed for a fixed heavy-element mixture at five values for the hydrogen mass fraction and three metallicities. An interpolation routine was written to compute EOS quantities for varying hydrogen mass fractions ($X = 0$ to $X = 0.8$) and metallicities ($Z = 0$ to $Z = 0.04$). The range of the tabulated data in temperature and density is suitable for modeling stars more massive than 0.8 $M_\odot$ lying on or above the main sequence in a Hertzsprung-Russell diagram. The tables themselves are not printed with this paper. Instead, these and the interpolation code are available by sending an e-mail request to opal@coral.llnl.gov or fswenson@lanl.gov. We anticipate full publication of the tables (28 Mbyte), the interpolation code, and this paper in a forthcoming AAS CD-ROM.

Because of the rather uncommon formulation of the OPAL EOS, we first discuss EOS methods that are more familiar to astrophysicists (§ 2) and then present (briefly) the activity-expansion formalism used in the OPAL EOS (§ 3). Details of the EOS tables and their use are presented in § 4, and a brief discussion of some applications as well as comparisons with other EOS results are given in § 5.

2. COMMONLY USED EQUATION-OF-STATE METHODS

In addition to the Saha equation, two other methods are frequently used to calculate stellar EOSs. Eggleton, Faulkner, & Flannery (1973, EFF) developed an EOS that is computationally simple and suitable for on-line use. They introduced an ad hoc free-energy term to produce pressure ionization at high density, i.e., when the interparticle separation is less than a bohr. This overcomes a well-known shortcoming of the Saha equation that predicts 30% neutral hydrogen in the solar center. Similar to Saha, EFF assume that ions and atoms are in their unperturbed ground states. The EFF method is relativistic and accounts for Fermi-Dirac statistics for electrons. However, it ignores Coulomb interactions and treats heavy elements as if they were always fully ionized. Additionally, it can produce unphysical phase transitions when used outside its range of validity. Because of these simplifications, the EFF EOS is computationally speedy. The EFF EOS also has the advantage that changes in compositions can easily be accommodated.

In view of the need for higher accuracy in the EOS, a number of attempts have been made to improve the EFF treatment. Christensen-Dalsgaard (1991), Christensen-Dalsgaard & Däppen (1992), and Swenson et al. (1996b) have added a Debye-Hückel free-energy term to the EFF model. This revision is known as the CEFF equation, to indicate that the Debye Coulomb correction has been added (see also Pols et al. 1995). Swenson & Rogers (1992) adjusted parameters in a CEFF EOS in order to obtain improved agreement with the activity-expansion (physical picture) method of Rogers (1994). A version of the EFF EOS that remedies many of the original shortcomings is currently being developed (Swenson, Rogers, & Irwin 1996a).

Going beyond the simple models to include the excited states and more correct Coulomb-interaction terms is fraught with difficulties. For example, the internal partition function for an isolated atom is divergent, so some method for cutting off the partition function must be introduced. Typically, this is accomplished by the assumption that the presence of other particles in the vicinity of a given atom (ion) confines the particle to a sphere of order of the ion-sphere radius or that it interacts with the plasma through a short-range, screened potenital, e.g., the Debye-Hückel potential. The resulting free energy is finite but discontinuous at plasma conditions in which a bound state is just entering the continuum. This behavior cannot be present in physically consistent models.

Mihalas, Hummer, and Däppen (Hummer & Mihalas 1988; Mihalas, Däppen, & Hummer 1988; Däppen et al. 1988; Däppen, Anderson, & Mihalas 1987; hereafter, collectively, MHD) have presented an occupation-probability formalism that is thermodynamically consistent and produces continuous free energies. It is commonly referred to as the MHD EOS. Relying on inferences from experimental measurements of level shifts (Goldsmith, Griem, & Cohen 1984), they postulated that the bound states of atoms and ions are unshifted by the plasma environment. They used a configurational free energy that depends explicitly on the occupation numbers of the individual states to define an occupation probability ω_i. The occupation probability gives an estimate of the number of bound states of type i that are available to be occupied. The quantity $1 - \omega_i$ is, thus, a measure of the fraction of total states that have been severely affected by plasma perturbations and no longer behave as localized states. In the case of neutral particles, the MHD approach uses the free energy of a parameterized hard-sphere gas to determine the occupation probability. For ion-ion interactions, the electric microfield (Stark-ionization theory) is used to determine the occupation probability. For ion-neutral interactions, they proposed the use of a combination of the two forms. The method is thus phenomenological but uses experimental data to fit free parameters in the occupation probability function. The MHD method has been used in numerous stellar-modeling sensitivity studies. For example, Christensen-Dalsgaard & Däppen (1992) reported generally good results whereas, using a different inversion method and studying deeper layers of the Sun, Dziembowski, Pamyatnykh, & Sienkiewicz (1992) reported significant differences between observation and the results of calculations that employ the MHD EOS. See § 5 for a brief comparison between OPAL and MHD results.

3. THE ACTIVITY-EXPANSION METHOD

Fundamental, many-body, quantum statistical treatments of the EOS of partially ionized plasmas start from the grand canonical ensemble (Hill 1956). In this approach, one views the system in terms of its fundamental constituents. The standard procedure for neutral gases is to expand the pressure in terms of two-body, three-body clusters, etc., i.e., a cluster expansion. The same is true for plasmas, but the long range of the Coulomb potential introduces substantial complications. In addition, the quantum nature of electrons introduces degeneracy and exchange corrections. The attractive electron-ion interaction leads to short-distance divergences in classical cluster coefficients, so the use of quantum mechanical methods is essential. Graphical resummation procedures can be used to remove the long-range divergences occurring in all cluster coefficients of plasmas. Composite particles (i.e., ions, atoms, and

© American Astronomical Society • Provided by the NASA Astrophysics Data System

1996ApJ...456..902R

molecules) arise naturally in the physical picture, so many-body effects on the bound states are determined from theory. This is an advantage over chemical-picture methods in current use, all of which introduce ad hoc models to obtain these effects. A detailed description of the procedure is given elsewhere (Rogers 1994, 1986, 1981; Kraeft et al. 1986; Dashen, Ma, & Bernstein 1969).

Important differences between a typical chemical-picture calculation and the physical picture can be illustrated with a simple example. Consider the hydrogen ionization equilibrium:

$$e^- + p^+ \leftrightarrow \mathrm{H} .$$

The typical free-energy minimization method (neglecting electron degeneracy) would adopt the following free-energy expression (e.g., Stix & Skaley 1990):

$$\frac{F}{kT} = -N_e \ln\left(\frac{eg_e}{n_e \lambda_e^3}\right) - N_p \ln\left(\frac{eg_p}{n_p \lambda_p^3}\right) - N_{\mathrm{H}} \ln\left(\frac{eg_{\mathrm{H}}}{n_{\mathrm{H}} \lambda_{\mathrm{H}}^3} Z_{\mathrm{int}}\right) + \frac{F_{\mathrm{DH}}}{kT} , \quad (1)$$

where

$$Z_{\mathrm{int}} = \sum_{nl} e^{-E_{nl}/kT} , \quad (2)$$

$$\frac{F_{\mathrm{DH}}}{kT} = \frac{V}{12\pi\lambda_{\mathrm{D}}^3} , \quad (3)$$

$$\lambda_{\mathrm{D}} = \left[\frac{kT}{4\pi e^2 (n_e + n_p)}\right]^{1/2} . \quad (4)$$

The first three terms on the right side of equation (1) correspond to the translational free energies for electrons, protons, and hydrogen atoms, with N_e, N_p, and N_{H} the corresponding number densities. Z_{int} is the sum over states (internal partition function), F_{DH} is the Debye-Hückel free-energy correction, and λ_{D} is the Debye screening length. Frequently, F_{DH} is reduced by a factor $\tau(x)$, introduced to account for the finite size of the ions (Graboske, Harwood, & Rogers 1969; MHD). However, this term is only appropriate for very hot, dense plasmas and is not valid outside a limited regime. It is well known that Z_{int} is divergent for an isolated ion; thus, some ad hoc mechanism must be introduced to truncate the sum. In practice, there are a number of ways this can be done. For example, a temperature-density–dependent, screened potential can be employed. But this type of truncation mechanism causes Z_{int} to change discontinuously at conditions in which a state moves into the continuum and is no longer counted. Therefore, equation (1) is intrinsically physically inconsistent.

In contrast, the analogous free energy that results from the many-body diagrammatic approach, to terms of order $(n_e^2)^{3/2}$ in the coupling parameter, is (Rogers 1994, 1990, 1986)

$$\frac{F}{kT} = -N_e \ln\left(\frac{eg_e}{n_e \lambda_e^3}\right) - N_p \ln\left(\frac{eg_p}{n_p \lambda_p^3}\right) - N_{\mathrm{H}} \ln\left(\frac{eg_{\mathrm{H}}}{n_{\mathrm{H}} \lambda_{\mathrm{H}}^3} Z_{\mathrm{int}}^{\mathrm{PL}}\right) + \frac{F_{\mathrm{DH}}}{kT} , \quad (5)$$

where

$$Z_{\mathrm{int}}^{\mathrm{PL}} = \sum_{nl} (2l+1)(e^{-\beta E_{nl}} - 1 + \beta E_{nl}) \quad (6)$$

is the so-called Planck-Larkin partition function. As described in Rogers (1981, 1986), the energy levels that appear in $Z_{\mathrm{int}}^{\mathrm{PL}}$ are unscreened except for high-lying states near the plasma continuum. The states that are screened change smoothly with plasma conditions. As a result, $Z_{\mathrm{int}}^{\mathrm{PL}}$ is both finite and a continuous function of temperature and density (although the density dependence is very slight for normal stellar conditions). It is important to note that the difference $Z_{\mathrm{int}} - Z_{\mathrm{int}}^{\mathrm{PL}}$ reflects a double counting of states in equation (4); i.e., the many-body treatment shows that this part of the internal partition function is included in the Debye-Hückel free energy. The MHD EOS displays a similar property through the use of the occupation-probability formalism but differs in significant details (Rogers 1990). The inconsistent Z_{int} used in MHD, however, has little influence at solar conditions.

Equation (5) is itself insufficient for the precise modeling of hydrogen at solar conditions. For this purpose, degeneracy, exchange, and quantum-diffraction corrections must be considered. The inclusion of these additional effects in the pressure of a fully ionized plasma (after elimination of the activities) yields

$$\frac{P}{kT} = \frac{n_e I_{3/2}(\alpha_e)}{I_{1/2}(\alpha_e)} + n_p + \frac{P_{\mathrm{ex}}}{kT} + \frac{P_{\mathrm{DH}}}{kT} f_p(\gamma_{ee}, \gamma_{ei}) , \quad (7)$$

where the $I_{n/2}$ functions are the Fermi functions, $\alpha_e = \mu_e/kT$ is the degeneracy parameter,

$$\frac{P_{\mathrm{ex}}}{kT} = \frac{2\pi}{3V} \int r^2 \left(\frac{e^2}{r}\right) [g_{ee}(r) - 1] \, dr \quad (8)$$

is the first-order electron exchange, g_{ee} is the electron-electron pair distribution function, and P_{DH} is the Debye-Hückel pressure correction, except that now the Debye length is corrected for electron degeneracy by use of

$$\lambda_{\mathrm{D}} = \left\{\frac{kT}{4\pi e^2 [n_e I_{-1/2}(\alpha_e)]/I_{1/2}(\alpha_e) + n_p}\right\}^{1/2} . \quad (9)$$

The factor $f_p(\gamma_{ee}, \gamma_{ei})$ in equation (7) is a quantum-diffraction correction to the classical Debye-Hückel pressure with γ_{ee} and γ_{ei} the diffraction parameters involving the ratio of the thermal de Broglie wavelength in relative coordinates to the Debye length (Rogers 1981). The first-order exchange correction (eq. [8]) is frequently omitted in astrophysical EOS calculations (EFF; MHD; Stanerio 1988; Stix & Skaley 1990), but in view of the current need for high precision, it must be included. Note that Landau & Lifshitz (1958) derived an incorrect expression for the effects of electron degeneracy on the classical Debye-Hückel free energy, which was corrected by Kidder & DeWitt (1961; see eqs. [3] and [9] of this work).

Not shown in equation (7) are a series of higher order exchange and Coulomb corrections that are intertwined with degeneracy and diffraction effects. These additional terms become important for plasma conditions that are more strongly coupled than solar or when extreme accuracy is needed, as in the analysis of helioseismic data. These terms are quite intricate, and they have produced some controversy. The works of DeWitt et al. (1995) and Alastuey & Perez (1992) agree to terms of order $(n_e^2)^2$ but differ in the term of order $(n_e^2)^{5/2}$. However, Alastuey & Perez (1995, private communication) have recently obtained agreement with DeWitt et al. In the treatment of multicomponent plasmas, the OPAL EOS uses a combination of exact theory and an approximate effective-potential method

© American Astronomical Society • Provided by the NASA Astrophysics Data System

1996ApJ...456..902R

to include diffraction corrections (Rogers 1994). This procedure does not include terms beyond Montroll-Ward that contribute at higher order. In the case of hydrogen, this procedure agrees with the recent work through the $(n_e^2)^2$-order correction.

The many-body diagrammatic perturbation methods, while being rigorous, are as a practical matter limited to weak coupling. However, the fact that ions behave classically allows an all-order summation of the ion-ion interaction terms (Rogers 1981). Quantum diagrammatic procedures are used to calculate terms to order $(n_e^2)^{5/2}$ for electron-electron and electron-ion terms (DeWitt 1966). These higher order terms incorporate additional Coulomb correlations and effects due to the finite size of composite particles. (The latter is a generalization of the $\tau(x)$ function previously mentioned.) The method is thus capable of including the main contribution due to strong coupling from the heavy-element admixture in hydrogen-helium plasmas. Although a pseudopotential method for going to higher order in the electron-electron and electron-ion interaction has been proposed (Rogers 1979), it has not been incorporated in this work.

For comprehensiveness, we now summarize the physical processes or phenomena modeled in the OPAL EOS: nonrelativistic Fermi-Dirac electrons, classical ions, all stages of ionization and excitation, molecular hydrogen, degenerate Coulomb corrections, quantum electron diffraction, electron exchange, pressure ionization, and terms arising from the so-called ladder diagrams of full quantum theory.

4. RESULTS

In the present work we have concentrated on producing EOS data tables suitable for many astrophysical applications. Whereas, in opacity calculations, elements heavier than neon, particularly iron, can dominate answers, this is not the case for the EOS. The OPAL EOS is obtained by solution of a fully coupled, many-component set of activity equations. Hence, the computer-time requirements increase disproportionately with these heavier elements due to their complex atomic structures. Because of this, we have truncated the elemental abundances to include only elements up to neon. The abundances of heavier elements (by number fraction) have been added to the neon abundance. Table 1 lists the relative abundances of the heavy elements used in the EOS tables (i.e., ignoring hydrogen and helium).

We have tabulated data, as a function of temperature and density, for pressure, internal energy, entropy, and the following second-order quantities (Cox & Guili 1968):

$$\chi_T = \left(\frac{\partial \ln P}{\partial \ln T}\right)_\rho , \quad \chi_\rho = \left(\frac{\partial \ln P}{\partial \ln \rho}\right)_T , \tag{10}$$

$$\Gamma_1 = \left(\frac{\partial \ln P}{\partial \ln \rho}\right)_S , \quad \frac{\Gamma_2}{\Gamma_2 - 1} = \left(\frac{\partial \ln P}{\partial \ln T}\right)_S , \tag{11}$$

$$C_V = \left(\frac{\partial E}{\partial T}\right)_V , \quad \left(\frac{\partial E}{\partial \rho}\right)_T . \tag{12}$$

Additional secondary quantities can be accurately computed analytically from the tabulated quantities by use of various thermodynamic identities (see Cox & Guili 1968). Derivatives of secondary quantities can only be obtained through numerical differentiation of tabulated quantities.

The temperature-density range of the tabulated data is shown in Figure 1. Note that the tables actually use the dimensionless quantity $T_6 = T/10^6$ K to define the temperature. We have tabulated data for hydrogen mass fractions $X = 0.0$, 0.2, 0.4, 0.6, 0.8 and for heavy-element mass fractions $Z = 0.00$, 0.02, 0.04 (corresponding helium mass fractions are given by $Y = 1 - X - Z$). An auxiliary code for interpolation in the variables T_6, ρ, X, and Z is available (see § 1).

TABLE 1

METALLIC COMPOSITION OF EOS TABLES

Element	Relative Mass Fraction	Relative Number Fraction
C	0.1906614	0.2471362
N	0.0558489	0.0620778
O	0.5429784	0.5283680
Ne	0.2105114	0.1624178

Figure 1 also shows temperature-density tracks for stars of various masses. Stars with masses of $\sim 0.8\ M_\odot$ or less fall outside the range of the data over part of their tracks. The tracks have two line types; solid curves indicate the radiative portion of the model star, and dashed curves indicate the convective portion. Of course, for stellar-evolutionary calculations, accurate EOS data is needed throughout the model. The division of the tracks into radiative and convective regions was made to illustrate that OPAL opacity tables are not limited to stars with masses above $0.8\ M_\odot$ since accurate opacity data is only needed in radiative regions (except in superadiabatic regions found in stellar surface regions).

The tables have a jagged edge toward high densities and low temperatures (see Fig. 1). This is the result of the attempt to

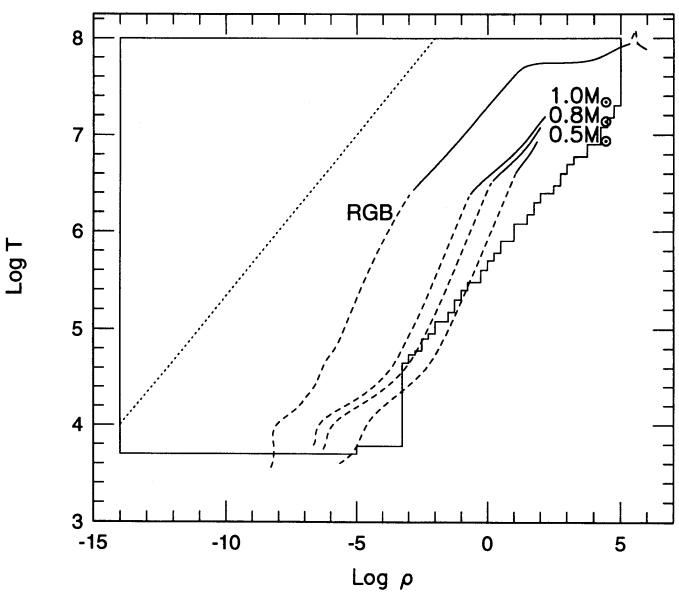

FIG. 1.—Temperature-density range covered by the EOS tables. Table points to the left of the dotted line may not be in strict local thermodynamic equilibrium. They are tabulated mostly for the convenience of having nearly square tables. The temperature-density points taken from three main-sequence stellar models at an age of 4.7×10^9 yr are indicated by their respective masses in the figure. The track of a $1\ M_\odot$ model near the end of red giant branch evolution is also plotted (identified by "RGB" in the figure). All of the models start with the initial solar composition. For these model tracks, solid lines indicate radiative regions, and dashed lines indicate convective regions. See § 4 for discussion.

© American Astronomical Society • Provided by the NASA Astrophysics Data System

1996ApJ...456..902R

limit the plasma conditions to weak electron coupling, where we are confident that the physics employed is well within its limits of validity. Extension of the tables to cover stars down to masses of $\sim 0.25\ M_\odot$ is currently being considered. The EOS tables cannot be extended to much higher temperatures because at 10^9 K electron pair production becomes a significant factor, and this is not modeled in the current OPAL EOS. We are also limited to densities below 10^5 g cm^{-3}, where electrons are nonrelativistic. Inclusion of the relativistic corrections for the electrons due to their quantum and Coulombic interactions will be very difficult. It will also be very difficult to extend the tables to lower temperatures, i.e., below 5000 K. There, the main difficulty is numerical, as the OPAL EOS has to solve for the electron density as part of its iteration procedure. When the electron density falls to very low values, this procedure has trouble converging and eventually fails. Thus, a new solution technique would have to be devised. Given that plasma conditions are likely to be nearly ideal (for the densities of interest), it may be more efficient to switch to a chemical picture, such as that of MHD or an improvement on EFF for atmospheric EOS data.

A preliminary version of these EOS tables was presented in Rogers (1994). Kosovichev (1995) used these preliminary tables in helioseismic inversion studies to deduce the helium abundance in the convection zone. He found that the OPAL EOS yields more physically consistent results than those obtained with MHD's. In somewhat similar helioseismic studies, Basu & Antia (1995) also obtained consistent results with the OPAL EOS. Nonetheless, both studies noted that the OPAL interpolated data was not smooth and cited a need for tabulation of the data on a more finely spaced temperature-density grid.

In the current work, we have constructed tables in the same temperature-density range but with triple the number of temperature points and double the number of density points used in the earlier work (Rogers 1994). The resultant tables are thus denser than the recommendations of Dorman, Irwin, & Pedersen (1991), who examined the impact of EOS tabular density on stellar-evolutionary models. In order to minimize computer requirements, this change was not accomplished by recomputation of the additional points with the OPAL EOS. Instead, we interpolated the additional values by use of the earlier tables and a version of the improved EFF EOS (Swenson et al. 1996a). Because the improved EFF EOS differs from the OPAL results by only a few percent or less, we were able to do simple interpolations in the ratios of OPAL to EFF quantities. This worked extremely well, judging from our comparisons of a few hundred interpolated points with computed OPAL values. This approach, while quite robust, is probably too slow for on-line use in stellar-model calculations. The tables are now sufficiently dense that interpolated values are both accurate and smoothly varying (although further refinement may be needed when modeling the most discriminating helioseismological data; see also § 5).

5. DISCUSSION

The EOS tables described herein are the first to be made available for astrophysical applications based on the physical-picture approach. Furthermore, the same computer code has been used to compute Rosseland mean opacities, thus making it possible to compute stellar models based on physically consistent EOSs and opacity data. While obviously desirable, this consistency between the EOS and opacity models has not been generally possible. The tables are sufficient for most modeling needs for stars more massive than $0.8\ M_\odot$ (see Fig. 1).

Even though we have performed a rigorous calculation for the conditions covered by these tables, we point out that the results for conditions less severe than solar (i.e., higher temperatures for a given density) will for the most part differ little from those obtained with a CEFF or MHD type of EOS. The possible exception is in regions of partial ionization, where such effects as pressure ionization (which has always been treated in an ad hoc fashion, until now) can play a significant role. Such effects are unlikely to be large enough to affect global model results. However, results that are sensitive to secondary thermodynamic quantities, such as Γ_1 or the adiabatic gradient, could be affected. Examples are stellar pulsations and pre–main-sequence lithium burning (Swenson et al. 1994b). However, those who may have been using overly simplistic models for their EOS data could see more dramatic changes.

Some isochoric comparisons of the several EOS methods described previously (§ 2) have been carried out by Däppen (1992). For stellar-envelope conditions, he found differences of a few percent in the derivatives of the EOS (eqs. [10]–[12]) given by the EFF and MHD approaches, but generally an order of magnitude less difference between OPAL and MHD. In regions where the Coulomb coupling is outside the range of validity of the Debye-Hückel theory, differences between MHD and OPAL become significant. Nevertheless, the MHD and OPAL EOSs have been found to give somewhat better agreement with observational data than the simple EFF model (Christensen-Dalsgaard & Däppen 1992).

It is beyond our intent to conduct extensive comparisons between the OPAL results and those of other EOSs. Nevertheless, we have chosen to make an illustrative comparison with the MHD calculations. It is also not our purpose here to make detailed characterizations of the EOS results. Once again, we

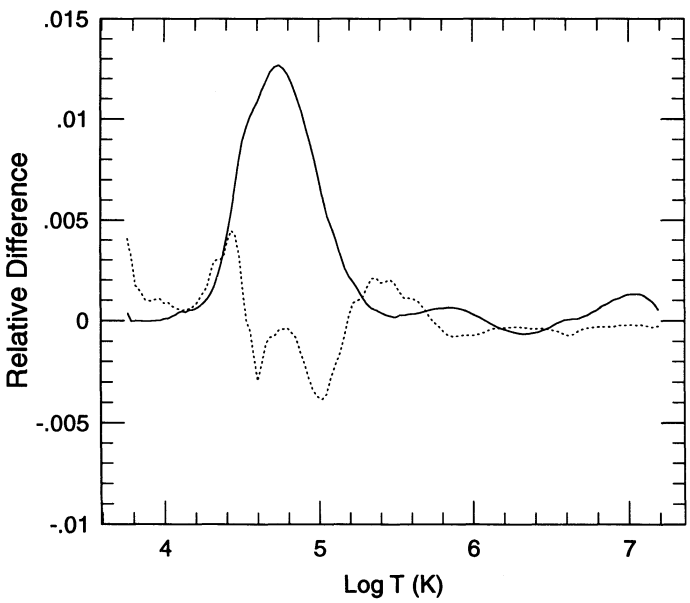

FIG. 2.—Comparison between OPAL and MHD results for solar conditions. Plotted are the relative differences in the pressure (*solid line*) and the secondary thermodynamic quantity Γ_1 (*dotted line*)—i.e., either $(P_{\rm MHD} - P_{\rm OPAL})/P_{\rm OPAL}$ or $(\Gamma_{1,\rm MHD} - \Gamma_{1,\rm OPAL})/\Gamma_{1,\rm OPAL}$. These quantities were computed by use of the run of density, temperature, and hydrogen mass fraction X from a solar model. The metal mass fraction Z is 0.02.

© American Astronomical Society • Provided by the NASA Astrophysics Data System

1996ApJ...456..902R

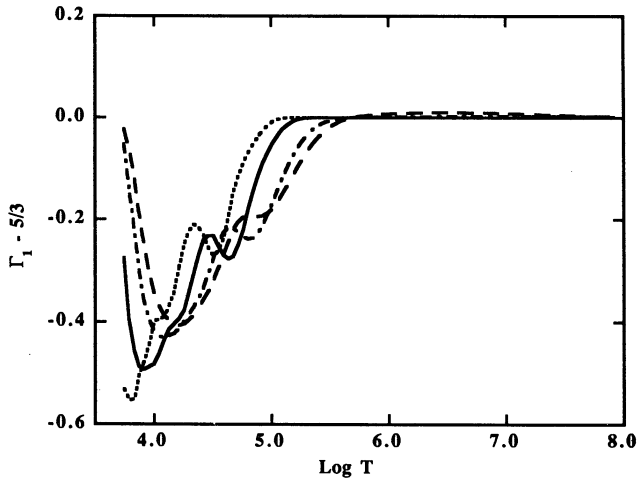

FIG. 3a

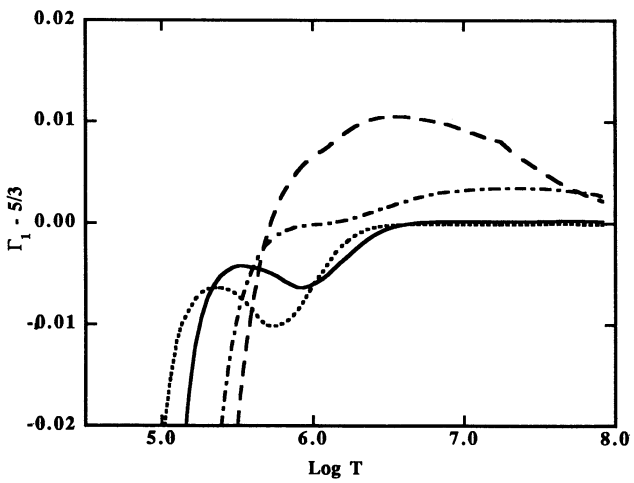

FIG. 3c

FIG. 3.—(*a*) $\Gamma_1 - \frac{5}{3}$ vs. T for hydrogen mass content $X = 0.4$ and helium mass content $Y = 0.6$. *Dotted line:* log $R = -5$; *solid line:* log $R = -3$; *dot-dashed line:* log $R = -1$; *dashed line:* log $R = 0$ ($R = \rho/T_6^3$, where T_6 is the temperature in 10^6 K). (*b*) Same as (*a*), but for reduced temperature range. (*c*) Same as (*b*), but for $X = 0.4$, $Y = 0.58$, and $Z = 0.02$.

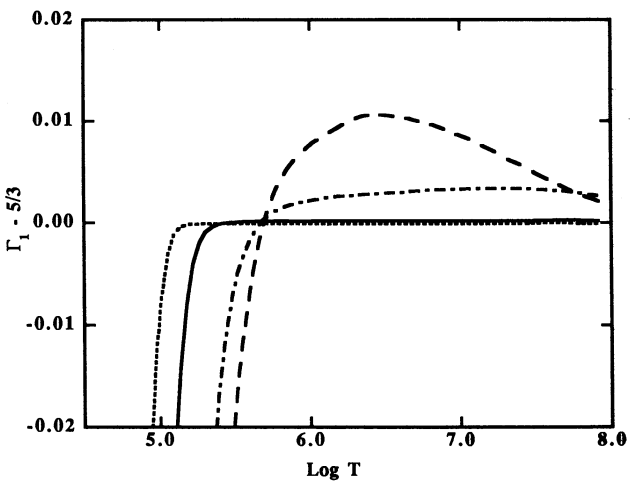

FIG. 3b

only give one illustrative example. For these examples, we concentrate our attention on solar conditions, as these are of interest because, in part, of the very detailed and precise observational data that has been and is being collected by numerous researchers.

Figure 2 shows the difference between computed values of the pressure and Γ_1 between the OPAL and MHD EOSs along a temperature-density track taken from a solar model (Swenson et al. 1994a). The comparison between physics predictions cannot be directly made here, as two different heavy-element mixtures were used. The MHD results were calculated with carbon, nitrogen, oxygen, and iron. However, we have performed some test calculations that indicate that pressure differences caused by the compositional difference alone are generally much less than 0.2% for solar conditions. Thus, we believe that the pressure difference of 1.2% at $\sim$50,000 K is mainly due to physics differences in the two approaches. We speculate that this difference can be attributed to the very different treatments of the interaction of the plasma with orbital electrons, in particular pressure ionization. The "pressure spike" displayed by the MHD model may be an indication that their phenomenological treatment of such effects is not valid over all regions of solar interest. This spike could be responsible for Kosovichev's (1995) failure to achieve physically self-consistent results when using the MHD EOS to model certain features of the solar oscillation spectrum.

Helioseismic modes are sensitive only to the deviations of Γ_1 from the ideal-gas value of $\frac{5}{3}$. Consequently, even small differences in this quantity substantially affect the agreement with the p-mode data. As shown in Figure 2, the difference between the MHD and OPAL results for this quantity generally vary between 0.1% and 0.5%. However, once again the compositional difference complicates the comparison. In this case, we have found it difficult to distinguish differences in Γ_1 due to composition from those due to physics. Thus, we make no conclusion about these differences but instead make some brief comments regarding the effects of compositional changes on the OPAL results.

Figures 3*a* and 3*b* show $\Gamma_1 - \frac{5}{3}$ versus log T at several values of log R ($R = \rho/T_6^3$) for a simple mixture of hydrogen and helium. Figure 3*a* shows results for the full range of the tables while Figure 3*b* is limited to the high-temperature range, above 100,000 K. The large negative deviations from $\frac{5}{3}$ at low temperatures in Figure 3*a* are due to the formation of ions and atoms. In the few-hundred-thousand kelvin range, the negative deviation due to bound complexes is competing with the positive deviations caused by Coulomb interactions. The positive Coulomb deviations start to dominate with increasing values of log R. Figure 3*c* is similar to Figure 3*b*, but includes metals. The small amount of high-Z admixture has a noticeable effect on the results. It is thus apparent that the modeling results for helioseismology will be sensitive to uncertainties in the abundances of heavy elements, e.g., uncertainties in neon impact in the million kelvin range near the base of the solar convective zone. This also illustrates the need for more detailed heavy-element mixtures in the construction of EOS tables for solar work. Currently, it is difficult to discriminate between different EOS models since superior agreement could be due to a fortuitous choice for the heavy-element mixture.

Recent studies have revealed the great sensitivity of the analysis of helioseismic data to derivatives of the EOS. This, combined with the high precision of the solar data currently being acquired, suggests that the neglect of heavier elements

© American Astronomical Society • Provided by the NASA Astrophysics Data System

1996ApJ...456..902R

may significantly impact inversion results (Kosovichev 1995; Basu & Antia 1995). To allow for the modeling of new Global Oscillation Network Group helioseismic data (Ulrich, Rhodes, & Däppen 1995), specialized OPAL EOS calculations will be needed that cover the range of solar parameters, on a finer grid, including explicitly the heavier elements as well as several additional thermodynamic derivatives. We plan to make solar tables for this specific purpose in the near future (we will also include information on the electron density for those who are modeling the results of the somewhat less precise data now being collected by a variety of neutrino telescopes). There are also a number of interesting problems for low-mass stars, the outer layers of white dwarfs, and globular-cluster stars (see, e.g., Chaboyer & Kim 1995). The nonideal effects become much more pronounced for these higher density, relatively cool conditions, and the Debye-Hückel approximation becomes inadequate (actually predicting negative pressures in extreme cases). The systematic many-body, quantum statistical approach we have developed should be reliable in this region, and we hope to extend the tables in this direction.

We are very grateful to W. Däppen for many useful discussions of the physics differences between the MHD and OPAL EOSs. We are also grateful to H. M. Antia, V. A. Baturin, and A. G. Kosovichev for critical evaluations of an early version of the EOS tables. F. J. S. thanks Don A. VandenBerg for supporting some of this work from his operating grant from the Natural Sciences and Engineering Research Council of Canada. Work of F. J. R. and C. A. I. was supported under the auspices of the Department of Energy by Lawrence Livermore National Laboratory under contract W-7405-ENG-48.

REFERENCES

Alastuey, A. 1994, in IAU Colloq. 147, The Equation of State in Astrophysics, ed. G. Chabrier & E. L. Schatzman (Cambridge: Cambridge Univ. Press), 43
Alastuey, A., & Perez, A. 1992, Europhysics Lett., 20, 19
Basu, S., & Antia, H. M. 1995, MNRAS, submitted
Chaboyer, B., & Kim, Y.-C. 1995, ApJ, 454, 767
Christensen-Dalsgaard, J. 1991, in Lecture Notes in Physics, 388, Challenges to Theories of the Structure of Moderate-Mass Stars, ed. D. O. Gough & J. Toomre (Berlin: Springer), 11
Christensen-Dalsgaard, J., & Däppen, W. 1992, A&A Rev., 4, 267
Christensen-Dalsgaard, J., Duvall, T. L., Gough, D. O., Harvey, J. W., & Rhodes, E. J. 1985, Nature, 315, 378
Cox, J., & Guili, R. 1968, Principles of Stellar Structure (New York: Gordon & Breach)
Däppen, W. 1992, Rev. Mexicana Astron. Astrofis., 23, 1144
Däppen, W., Anderson, L., & Mihalas, D. 1987, ApJ, 319, 195
Däppen, W., Mihalas, D., Hummer, D. G., & Mihalas, B. W. 1988, ApJ, 332, 261
Dashen, R., Ma, S.-K., & Bernstein, H. J. 1969, Phys. Rev., 187, 345
DeWitt, H. E. 1966, J. Math. Phys., 7, 6169
DeWitt, H. E., Schlanges, M., Sakakura, A. Y., & Kraeft, W. D. 1995, Phys. Lett. A, 30, 326
Dorman, B., Irwin, A. W., & Pedersen, B. B. 1991, ApJ, 381, 228
Dziembowski, W. A., Pamyatnykh, A. A., & Sienkiewicz, R. 1992, Acta Astron., 14, 5
Ebeling, W. 1974, Physica, 73, 573
Ebeling, W., Kraeft, W. D., & Kremp, D. 1977, Theory of Bound States and Ionization Equilibrium in Plasmas and Solids (Berlin: Akademie)
Eggleton, P., Faulkner, J., & Flannery, G. P. 1973, A&A, 23, 261 (EFF)
Goldsmith, S., Griem, H. E., & Cohen, L. 1984, Phys. Rev. A, 30, 2775
Graboske, H. C., Harwood, D. J., & Rogers, F. J. 1969, Phys. Rev., 186, 210
Guenther, D. B., Demarque, P., Kim, Y.-C., & Pinsonneault, M. H. 1992, ApJ, 387, 372
Hill, T. L. 1956, Statistical Mechanics (New York: McGraw-Hill), chap. 5
Hummer, D. G., & Mihalas, D. 1988, ApJ, 331, 794
Iglesias, C. A., & Rogers, F. J. 1991a, ApJ, 371, L73
Iglesias, C. A., & Rogers, F. J. 1991b, ApJ, 371, 408
Iglesias, C. A., Rogers, F. J., & Wilson, B. G. 1987, ApJ, 322, L45
———. 1992, ApJ, 397, 717
Kidder, R. E., & DeWitt, H. E. 1961, J. Nucl. Energy C, 2, 218
Kosovichev, A. G. 1995, Adv. Space Res. 15(7), 95
Kraeft, W. D., Kremp, D., Ebeling, W., & Ropke, G. 1986, Quantum Statistics of Charged Particle Systems (New York: Plenum)
Krasnikov, Yu. G. 1977, Soviet Phys.—JETP Lett., 46, 271
Krasnikov, Yu. G., & Kucherenko, V. I. 1978, Teplofizika Vysokikh Temperatur, 16, 43
Landau, L. D., & Lifshitz, E. M. 1958, Statistical Physics (London: Pergamon)
Mihalas, D., Däppen, W., & Hummer, D. G. 1988, ApJ, 331, 815
Moskalik, P., Buchler, J. R., & Marom, A. 1992, ApJ, 385, 685
Pols, O. R., Tout, C. A., Eggleton, P. P., & Han, Z. 1995, MNRAS, submitted
Rogers, F. J. 1979, Phys. Rev. A, 19, 375
———. 1981, Phys. Rev. A, 24, 1531
———. 1986, ApJ, 310, 723
———. 1990, ApJ, 352, 689
———. 1994, in IAU Colloq. 147, The Equation of State in Astrophysics, ed. G. Chabrier & E. L. Schatzman (Cambridge: Cambridge Univ. Press), 16
Rogers, F. J., & Iglesias, C. A. 1992, ApJS, 79, 507
Saha, M. 1920, Philos. Mag., 40, 472
Simon, N. R. 1982, ApJ, 260, L87
Staniero, O. 1988, A&AS, 76, 157
Stix, M., & Skaley, D. 1990, A&A, 232, 234
Swenson, F. J., Faulkner, J., Iglesias, C. A., Rogers, F. J., & Alexander, D. R. 1994a, ApJ, 422, L79
Swenson, F. J., Faulkner, J., Rogers, F. J., & Iglesias, C. A. 1994b, ApJ, 425, 286
Swenson, F. J., & Rogers, F. J. 1992, BAAS, 24, 1176
Swenson, F. J., Rogers, F. J., & Irwin, A. W. 1996a, in preparation
Swenson, F. J., VandenBerg, D. A., Alexander, D. R., & Irwin, A. W. 1996b, in preparation
Ulrich, R. K., Rhodes, E. J., & Däppen, W., ed. ASP Conf. Proc. 76, Helio- and Astroseismology from the Earth and Space (ASP Conf. Ser., 76) (San Francisco: ASP)

© American Astronomical Society • Provided by the NASA Astrophysics Data System